Precise correlation energies in small parabolic quantum dots from configuration interaction

S. A. Blundell*
Service de Physique Statistique, Magnétisme et Supraconductivité, INAC, CEA-Grenoble/DSM, 17 rue des Martyrs, F-38054 Grenoble Cedex 9, France

K. Joshi†
Center for Modeling and Simulation, University of Pune, Ganeshkhind, Pune 411 007, India
(Received 22 December 2009; revised manuscript received 16 February 2010; published 19 March 2010)

We calculate precise correlation energies of ground and low-lying excited states in circular parabolic quantum dots containing $N=2-20$ electrons by means of a configuration interaction (CI) method with a numerical, mean-field basis set. All excitations are allowed for $2\leq N\leq 7$ (full CI), while up to hextuple excitations are included for $N=8,9$, and up to pentuple excitations for $10\leq N\leq 20$. The energies are extrapolated to the limit of basis-set completeness and the truncation error due to restricting the number of Slater determinants is monitored. For high electron densities (Wigner-Seitz radius $r_s\approx 1.7a_0^*$), the approach achieves errors of order 0.3 mHa* for $N=3$, a few mHa* for $N=6-9$, rising to about 100 mHa* for $N=20$. A comparison is made with recent quantum Monte Carlo calculations.

DOI: 10.1103/PhysRevB.81.115323 PACS number(s): 73.21.La, 73.21.Fg, 68.65.Hb, 68.65.Fg

I. INTRODUCTION

Semiconductor quantum dots[1,2] are formed when a finite number of free carriers (electrons or holes) are confined electrostatically to dimensions of order nanometers. The number of confined electrons can vary from a few to several hundred, with smaller numbers of electrons becoming increasingly technologically important in nanometer-sized devices such as the single-electron transistor[3] (SET). In a large class of devices of practical importance, as well as in many experiments in mesoscopic physics, one deals with a confined electron system that is essentially two dimensional (2D), having lateral dimensions (x and y dimensions) of order tens or hundreds of nanometers but a thickness (z dimension) of order only a few nanometers. Such an electronic system can be produced by using a suitable arrangement of gate electrodes to confine laterally the 2D electron gas that is formed close to the interface between two semiconductors or between a semiconductor and an insulator.[4] Alternatively, they can be created in an etched vertical pillar structure of thin layers of different semiconductors.[5,6]

Since the typical de Broglie wavelength in semiconductors is of the order of tens of nanometers, confinement on this scale leads to discrete energy levels, and atomiclike properties such as shell effects, so that the systems are often referred to as *artificial atoms*. For instance, particularly stable systems are found for "magic" numbers of confined electrons corresponding to filled fermionic shells.[7] Just as with atoms, molecules, or nuclei, a theoretical approach to these systems requires a careful treatment of finite-size quantum many-body (correlation) effects.

In this paper, we describe a calculation of the correlation energy in small quantum dots (containing up to 20 electrons) and compare to other, precise calculations in the literature. We make two basic approximations that are common in the field.[8] First, the quasi-2D approximation, in which we assume that the system is always in the lowest-energy state or subband for quantization along the z axis, so that the equations describing the system can be effectively reduced to two dimensions. Second, we describe the confined electrons in the conduction band of the semiconductor by an effective mass approximation, assuming a single effective mass m^* for the conduction band and a dielectric constant ϵ. In addition, the external confinement potential is taken to be circular parabolic.

Using this model of a quasi-2D quantum dot, several electronic-structure methods have been considered in the literature, including Hartree-Fock[9] (HF), Brueckner-Hartree-Fock,[10] spin-density functional theory[11–15] (SDFT), quantum Monte Carlo[16–21] (QMC), configuration-interaction[2,22–30] (CI), and coupled cluster.[31–33] In this work we use a CI approach.

Most CI calculations for semiconductor quantum dots have in practice been based on simple-harmonic-oscillator (SHO) basis sets. These have the convenience of a simple analytic form, together with analytic formulas for Coulomb and other matrix elements. Although it is always possible within this framework to perform CI calculations with respect to HF ground states, for example, by re-expanding the HF basis states in terms of SHO states, additional computation is thereby required in the CI phase of the calculation. We use instead a CI method in which the basis set is generated numerically, and stored, on a 2D Cartesian grid for an arbitrary mean-field potential. Real-space methods such as this have been used before in the context of CI.[28,30,34] By combining this approach with a careful extrapolation to the limit of basis-set completeness, we extract ground-state and excitation energies for small quantum dots (containing $2\leq N\leq 20$ electrons) with a globally better precision than previously reported for CI on this problem.

Aside from the inherent interest of semiconductor quantum dots, one can also regard the quasi-2D parabolic dot as a simple model system in which to test electronic-structure methods, characterized by many strongly interacting, nearly degenerate configurations. In the case of quantum dots, the benchmark electronic-structure method is often considered to be QMC. For instance, Pederiva *et al.*[20] report calculations of ground-state energies and excitation energies for $2\leq N\leq 13$

with a statistical error corresponding to several parts in 10^5 of the ground-state energy. But QMC methods can also contain systematic errors, which are harder to estimate within the approach. We therefore undertake a detailed comparison between the present method and QMC work.

The paper is organized as follows. Section II gives an overview of our calculation method. In the following section, we describe in some detail a few example calculations on small systems, in order to explain further aspects of our methodology. In Sec. IV we then make a detailed comparison with the QMC results of Ref. 20. The conclusions are given in Sec. V.

II. METHOD

A. Numerical basis set

We assume the electron gas to be quasi-two-dimensional and wish to solve for the many-body envelope wave function in the effective mass approximation.[8] The N-electron Hamiltonian is

$$H = \sum_{i=1}^{N} \left[-\frac{\nabla_i^2}{2m^*} + V_{\text{ext}}(\mathbf{r}_i) \right] + \sum_{i<j}^{N} \frac{e^2}{(4\pi\epsilon_0)\epsilon|\mathbf{r}_i - \mathbf{r}_j|}, \quad (1)$$

where m^* is the effective mass in the conduction band of the semiconductor, ϵ is the dielectric constant, $V_{\text{ext}}(\mathbf{r})$ is the external confining potential, and the vector $\mathbf{r}$ is two dimensional. In the applications reported here we assume a circular parabolic confinement potential

$$V_{\text{ext}}(\mathbf{r}) = \frac{1}{2} m^* \omega^2 r^2. \quad (2)$$

The many-body envelope wave function Ψ satisfies the Schrödinger equation

$$H\Psi = E\Psi. \quad (3)$$

We shall work in *effective* atomic units corresponding to scaled coordinates with lengths expressed in units of $a_0^* = (\epsilon/m^*)a_0$, where a_0 is the Bohr radius, and energies in units of $\text{Ha}^* = (m^*/\epsilon^2)$ Ha. One can thus effectively put $m^* = \epsilon = e = (4\pi\epsilon_0) = 1$ in Eq. (1) and, accordingly, we shall drop m^* and ϵ from all subsequent equations.

To solve Eq. (3), we use the CI approach,[35] in which the many-body wave function is expanded in terms of a set of Slater determinants Φ_α,

$$\Psi = \sum_{\alpha}^{M} c_\alpha \Phi_\alpha. \quad (4)$$

The Slater determinants are built out of a single-particle basis corresponding to a suitable mean-field approximation. The states (spin-orbitals) ψ_ℓ of this basis satisfy

$$h_0 \psi_\ell = \epsilon_\ell \psi_\ell, \quad (5)$$

$$h_0 = -\frac{\nabla^2}{2} + V_{\text{ext}} + U. \quad (6)$$

The potential U here is intended to be a mean-field potential that approximates the effect of the electron-electron interaction, but for the method it is in principle arbitrary. It can be a local potential, as in the effective potential $V_{\text{eff}}(\mathbf{r})$ of Kohn-Sham theory,[36] or nonlocal, as in the HF potential. It could also be spin dependent, although here we shall only consider spin-independent potentials U. Thus the spin-orbital solutions to Eq. (5) take the form

$$\psi_\ell = \varphi_k(\mathbf{r})\chi(m_s), \quad (7)$$

where $\chi(m_s)$ is a spin-1/2 eigenstate with z component of spin $m_s = \pm 1/2$, and the $\varphi_k(\mathbf{r})$ are *orbitals*, which also satisfy $h_0\varphi_k = \varepsilon_k\varphi_k$. To set up the CI equations, we generate numerically a set of orbitals φ_k from the ground state up to some upper energy cutoff ε_{cut}. The Slater determinants included in Eq. (4) are formed by distributing the N electrons among the available states ψ_ℓ such as to satisfy the Pauli exclusion principle, according to possible truncation schemes that are described in more detail below. Note that in the basis-set limit $\varepsilon_{\text{cut}} \to \infty$, and with the inclusion of all possible Slater determinants (that is, full CI), the energies tend to the same exact values independent of the basis-set potential U. However, for any given truncation there will be a residual dependence on U.

We use a numerical real-space approach in which all single-particle orbitals, and other quantities such as potentials, are represented on a 2D Cartesian grid. To generate a single-particle orbital basis $\varphi_k(\mathbf{r})$, we express the Laplacian in Eq. (6) in terms of high-order (typically 5, 7, or 9 point) centered finite differences.[37] The mean-field potential $U(\mathbf{r})$ as well as the external potential $V_{\text{ext}}(\mathbf{r})$ are at this stage assumed to be local and are also represented on the Cartesian grid. The single-particle Hamiltonian h_0 (6) is then a sparse matrix of dimension $N_g \times N_g$, where N_g is the total number of points on the 2D Cartesian grid. In practice, N_g can vary from about 10^3 to 10^5 depending on the application. The lowest (most negative) m eigenvalues and eigenvectors of h_0 may now be readily extracted by sparse matrix methods such as the Lanczos[38] or Davidson[39] algorithms (or by standard Lapack routines if N_g is sufficiently small, of order only several thousand). In this way, one can readily generate a basis set of several hundred (or several thousand) single-particle orbitals $\varphi_k(\mathbf{r})$ and eigenvalues ε_k on the 2D grid for arbitrary numerically defined external potentials and mean-field potentials.

We also wish to generate a basis set for a nonlocal potential such as the HF potential. For this purpose, we first generate several hundred to a thousand basis functions for a local mean-field potential such as the effective potential of Kohn-Sham theory,[36] using the algorithm described above. The HF equations (restricted or unrestricted) are then rewritten with the HF orbitals expanded in terms of these local orbitals, leading straightforwardly to an iterative solution. For this method to be accurate, it is necessary that rather more orbitals of the local mean field are used than the number of HF orbitals that are desired. For instance, if one desires 100 HF orbitals, it may be necessary to use upwards of 500 Kohn-Sham orbitals. It is straightforward to monitor the error caused by this truncation and we ensure that any errors

incurred are at least 1–2 orders of magnitude smaller than the truncation error in our final CI results due to the upper energy cutoff on the single-particle basis or to any truncations in the number of Slater determinants that we include. Note that because we store the final HF basis set on the 2D grid, the computational effort required in the subsequent CI calculation is independent of the number of Kohn-Sham orbitals that we use to compute the HF basis. The computer time required to converge the HF equations is typically negligible compared to the time spent on the CI calculation.

Coulomb matrix elements are evaluated as

$$\langle ab|r_{12}^{-1}|cd\rangle = \langle b|V_{ac}|d\rangle \delta(m_a,m_c)\delta(m_b,m_d), \tag{8}$$

where $V_{ac}(\mathbf{r})$ is the potential due to a 2D sheet of charge

$$V_{ac}(\mathbf{r}) = \int d^2r' \frac{\varphi_a^*(\mathbf{r}')\varphi_c(\mathbf{r}')}{|\mathbf{r}-\mathbf{r}'|}, \tag{9}$$

and the two Kronecker deltas give the spin selection rule for the conservation of s_z at each vertex of the Coulomb interaction. We evaluate the potential $V_{ac}(\mathbf{r})$ by regarding the expression (9) as a discrete convolution over the 2D Cartesian grid of a density $\rho_{ac}(\mathbf{r}')=\varphi_a^*(\mathbf{r}')\varphi_c(\mathbf{r}')$ with a Green's function $G(\mathbf{r},\mathbf{r}')=|\mathbf{r}-\mathbf{r}'|^{-1}$. The discrete convolution is handled by standard fast Fourier transform methods and grid doubling.[40] The approach is generalized by interpolating the density $\rho_{ac}(\mathbf{r}')$ between grid points by high-order interpolation formulas (at least cubic), to improve accuracy. The algorithm satisfies the *reciprocity* relation

$$\langle b|V_{ac}|d\rangle = \langle a|V_{bd}|c\rangle, \tag{10}$$

to machine precision, which is a useful property.

In the CI method,[35] one diagonalizes the many-body Hamiltonian (1) in the space of Slater determinants Φ_α. This yields a large, sparse Hamiltonian matrix H_{CI} that we diagonalize by the Lanczos or Davidson algorithms. In the present version of the code, the nonzero matrix elements of H_{CI} are stored in sparse-matrix format[37] in run-time memory, and it is the limit on the available memory that determines the maximum number of Slater determinants (configurations) that we include in the CI expansion (4). At present we include up to a few million configurations. To go beyond this would require either the use of disk storage, or the re-evaluation of the matrix elements of H_{CI} on the fly, as they are required on each iteration of the Lanczos or Davidson algorithm.

We reduce the grid error to negligible levels (typically less than 10^{-5} Ha* in energies) by choosing the grid spacing to be sufficiently small. Provided one uses a high-order finite-difference representation for the Laplacian and a high-order interpolation of the density in the Poisson solver, it is usually possible to keep the grid spacing relatively large. In the applications reported here, a grid spacing of around 0.5 a_0^* was used.

B. Hierarchy of CI truncations

A common approach to choosing the set of configurations included in the diagonalizaton of H_{CI} is to distribute the N electrons in all possible ways among the available single-particle states consistent with the Pauli exclusion principle. This gives the so-called "full CI" scheme, which includes configurations in which *all* electrons in the ground configuration are excited (up to the upper energy cutoff $\varepsilon_{\mathrm{cut}}$ in the single-particle basis). The error in the full CI approach arises only from the incompleteness of the single-particle basis (the upper energy cutoff $\varepsilon_{\mathrm{cut}}$).

In quantum chemistry[35] and atomic physics[41] applications it is common to use a truncated CI scheme based on the hierarchy of single, double, triple, …, etc., excitations of the ground configuration. This hierarchy is known in these fields to have reasonable convergence properties with respect to the degree of excitation, at least when a mean-field (typically a HF) basis is used. This opens the possibility of obtaining good accuracy from CI calculations for larger numbers of electrons by truncating at, say, double or quadruple excitations. This possibility has not been explored systematically in the context of quasi-2D quantum dots, and is one of our main interests in this paper.

Accordingly, we shall arrange our CI calculations hierarchically, including successively single, double, triple, …, etc., excitations of the ground configuration up to the full CI limit (for $N\leq 7$), in order to assess the convergence with respect to the rank of excitation for various basis sets. The excitation hierarchy has a straightforward definition when the ground state can be approximated by a single determinant; triple excitations, for instance, are simply the set of all configurations in which exactly three electrons are excited from the ground configuration. In the case of 2D circular parabolic quantum dots, a single-determinantal ground state is generally only appropriate for *magic* numbers of electrons ($N=2,6,12,20,\ldots$) corresponding to full shells of electrons in a shell model of the quantum dot.[7]

We also wish to discuss open-shell systems and therefore we consider a generalization of this hierarchy as follows. We suppose that the ground state can be approximated in lowest order by a linear combination of determinants forming a *model space*. Although there is some degree of arbitrariness in the choice of the determinants forming the model space, in the applications to be discussed here a convenient definition of the model space can be made in terms of a shell model of the quantum dot. An "open-shell" system is taken to consist of a closed-shell core of N_c electrons, together with N_v valence electrons distributed over M_v possible valence states (where $M_v > N_v$). The M_v valence states are typically either degenerate or nearly degenerate, so that configurations containing them may be expected to interact strongly with one another. We thus distinguish three classes of single-particle state: the N_c *core* states, which are occupied in the closed-shell core; the M_v quasidegenerate *valence* states; and the *excited* states, which consist of all remaining states.

The model space is taken to be the set of all configurations formed by distributing the N_v valence electrons in all possible ways among the M_v valence states. We then define the n-fold excitations in the CI hierarchy to consist of the set

TABLE I. Ground-state energy of the $N=6$ circular parabolic dot for $r_s=1.5a_0^*$ calculated by full CI using a variety of basis sets. Notation: KS, Kohn-Sham; HF, Hartree-Fock. Columns headed by a value of w denote use of the analytic potential $U(w,r)$ in Eq. (13) with that value of w. LO-CI denotes lowest-order CI (see text). Figures in parentheses are the estimated error (in the last tabulated digit) after extrapolation to the basis-set limit. Units: Ha*.

Approx.	KS	HF	$w=1$	$w=0.75$	$w=0.5$	$w=0.25$
LO-CI	9.3959	9.3909	9.4034	9.5500	9.8920	10.286
Singles	−0.0051	0.0000	−0.0127	−0.1918	−0.4858	−0.743(1)
Doubles	−0.3724(8)	−0.3746(7)	−0.3676(3)	−0.3027(7)	−0.2908(14)	−0.365(3)
Triples	−0.0211(1)	−0.0185(12)	−0.0249(1)	−0.0613(2)	−0.1155(5)	−0.159(4)
Quadruples	−0.0435(3)	−0.0435(3)	−0.0434(3)	−0.0377(4)	−0.0402(6)	−0.054(2)
Pentuples	−0.0022(7)	−0.0019(7)	−0.0026(10)	−0.0048(7)	−0.0082(10)	−0.012(2)
Hextuples	−0.0014(4)	−0.0014(4)	−0.0014(4)	−0.0013(5)	−0.0010(5)	−0.001(1)
TOTAL	8.9503(12)	8.9508(16)	8.9508(12)	8.9505(12)	8.9504(19)	8.952(8)

of configurations formed by exciting n electrons in all possible ways from all configurations in the model space (taking care to avoid double counting by excluding any configuration that is already present in the model space or that has already been included in a lower rank of excitation).

We denote by "lowest-order CI" (LO-CI) the diagonalization within the model space only. This corresponds to a rank zero of excitation according to the above scheme and is the lowest-order approximation possible within the truncated CI hierarchy.

C. Quantum numbers

Since the Hamiltonian (1) is spin independent, it follows that the many-body states can be classified according to a definite total spin. We require a CI eigenstate to be an eigenstate of the total z component of spin S_z by restricting to sets of Slater determinants each having a definite prechosen S_z eigenvalue (which is standard practice). In the open-shell procedure, the definition of the model space is similarly restricted by the choice of S_z eigenvalue. We then determine the total spin quantum number S of an eigenstate by acting on it with $\mathbf{S}^2$. When the external potential is circularly symmetric, as in the applications described in this paper, we make a similar further restriction of determinants to those having a definite value of total orbital angular momentum L_z. Note, however, that in order to be able to do this consistently, it is important that the mean-field potential U is also chosen to be circularly symmetric, so that the single-particle states, and therefore the Slater determinants, actually do have definite orbital angular momentum. This may require using an approximate or circularly averaged mean field U.

III. EXAMPLE CALCULATIONS

A. Closed-shell system: $N=6$ electrons

To explain further our methodology, we first consider the ground state of a circular parabolic quantum dot with $N=6$ electrons at near-equilbrium density $r_s=1.5a_0^*$. Following the useful convention of Koskinen *et al.*,[11] we here define the approximate average Wigner-Seitz radius r_s for a circular parabolic confining potential $V_{\text{ext}}(\mathbf{r})=\omega^2 r^2/2$ by

$$r_s^3=\frac{1}{\omega^2\sqrt{N}} \tag{11}$$

(in effective atomic units).

In the shell model of the quasi-2D quantum dot, the $N=6$ electron dot is a closed-shell system with a spin-zero ground state,[7] which is therefore well represented by a single-determinantal ground state. In Table I we show the full CI calculation of the ground-state energy organized hierarchically for increasing degree of excitation from the ground-state determinant. We define the contribution from n-fold excitations in this table (and later) as follows. Let E_n be the result of a CI calculation truncated at n-fold excitations, that is, containing the lowest-order (model) space of determinants together with single, double, …, up to n-fold excitations. Then we define the contribution ΔE_n of n-fold excitations to be

$$\Delta E_n=E_n-E_{n-1}. \tag{12}$$

The lowest-order (LO-CI) contribution, $\Delta E_0\equiv E_0$, is defined to be that resulting from diagonalizing the Hamiltonian over the model space only.

Results are given in Table I for several different basis sets corresponding to different mean-field potentials U. In addition to the Kohn-Sham (KS) effective potential $U=V_{\text{eff}}$ of DFT and the HF potential $U=V_{\text{HF}}$, we also consider an approximation to the mean-field potential with a simple analytical form. This potential is given by

$$U(w,r)=wV_0\exp(-\alpha r^2), \tag{13}$$

where V_0 is the potential at the center of a disk of uniform charge density $\sigma_0=1/(\pi r_s^2)$ containing N electrons,

$$V_0=\frac{2\sqrt{N}}{r_s}. \tag{14}$$

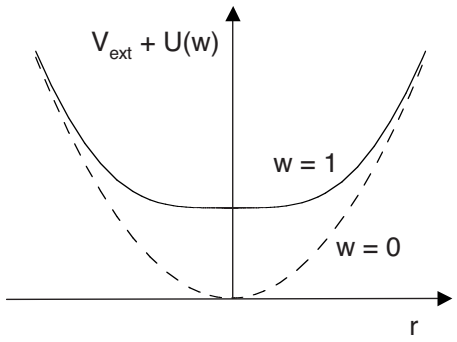

FIG. 1. Total potential $V_{ext}(r)+U(w,r)$ for the approximate analytical mean field $U(w,r)$ in Eq. (13). Solid line: full potential, $w=1$. Dashed line: bare external potential, $w=0$.

The parameter α in Eq. (13) is determined by requiring that the potential $U(1,r)$ cancel the second derivative of the external potential, which may be shown to lead to

$$\alpha = \frac{1}{4Nr_s^2}. \tag{15}$$

In this way, for $w=1$, the potential $U(w,r)$ has the effect of flattening the bottom of the parabolic confining well (see Fig. 1), which is an important effect of any reasonable mean-field potential. We further vary this potential by applying an overall scaling factor w, so that $w=1$ gives the optimally flattened total potential, while $w=0$ gives the bare external potential.

In Table I we have also attempted to extrapolate the results to the basis-set limit $\varepsilon_{cut}\to\infty$. To perform this extrapolation, we first perform a series of calculations in which the basis set is truncated after a number n_{sh} of full shells, with $n_{sh}=2,4,6,\ldots$, etc. A "full shell" is characterized by a small gap in the spectrum, and for our mean-field basis sets these generally occur for the same states as are found in the harmonic oscillator shell structure (except possibly at the highest energies). Then we perform fits of the energies to polynomials in $1/n_{sh}$ and extrapolate to $(1/n_{sh})\to 0$. An estimate of the error in this extrapolation is found by testing the consistency of the extrapolation as the number of points in the fit is varied. We offer no particular justification for this procedure other than that, after a certain amount of trial and error, it does seem to work quite well. It is in general important to choose only even (or only odd) values of n_{sh}, since there are often marked odd-even effects related to the alternating parity of successive shells. The result of the extrapolation is a small, but useful, additional contribution to each value tabulated.

From Table I we see that, as expected, each potential U that we consider leads to a final total energy (that is, at full CI level) in agreement to within the estimated uncertainty due to the extrapolation to the basis-set limit. This error is the only error in the calculation in the full CI limit. The estimated error for mean-field potentials in Table I is 5–6 times smaller than that for the nearly bare external potential ($w=0.25$). This occurs simply because a mean-field basis includes more of the physics in the lower-lying members of the basis set and hence produces a smaller truncation error at any given upper energy cutoff. Note that the calculation for each potential in Table I involves the same number of Slater determinants and hence an identical computational effort (within our approach, in which the numerical basis set is stored on the 2D grid). It is also possible to optimize a simple-harmonic basis set for full CI calculations, as done for instance in Ref. 26, by modifying the frequency parameter ω so as to gain some of the benefits of this effect.

TABLE II. Contributions to the ^3S ground-state energy of the $N=4$ electron circular parabolic dot with density parameter $\lambda=1.89$ ($r_s\approx 1.9a_0^*$). HF-av denotes a configuration-averaged Hartree-Fock basis set, $w=0.75$ a basis set in the potential of Eq. (13) with that value of w. Units: Ha*.

Excitation	HF-av	$w=0.75$
LO-CI	3.9268	3.9573
Singles	−0.0886	−0.1298
Doubles	−0.1131(4)	−0.1028(4)
Triples	−0.0100	−0.0095
Quadruples	−0.0011(1)	−0.0011
TOTAL	3.7141(4)	3.7141(4)
Ref. 20 (QMC)	3.7145(1)	

The advantage of a mean-field basis is more evident in *truncated* CI. The results in Table I show a pattern of convergence with respect to degree of excitation that is well known in quantum chemistry[35,42] and atomic physics[41] applications. It follows from the definition of the HF potential (via a result known as Brillouin's theorem),[35] and from the definition of ΔE_1 given in Eq. (12), that $\Delta E_1\equiv 0$ for the HF potential. To the extent that any reasonable mean field approximates the HF potential, the singles contribution is thus generally small. Another important feature of Table I is that, for mean-field potentials, quadruple excitations are generally at least as important as triple excitations. This result, which is found also in closed-shell atoms and molecules, occurs because in CI the quadruple excitations contain the effect of two disconnected pair excitations, which is often more important than triple excitations.[41,42] Thus, a truncation after quadruple excitations is generally more appropriate than one after triple excitations. Now, it follows from Table I that the doubles truncation error is 65 mHa* for a HF potential and 226 mHa* for the $w=0.25$ potential, while the quadruples truncation error is 3.4 mHa* for HF versus 12.7 mHa* for the $w=0.25$ potential. Once again, our numerical approach has the property that the computational effort required at any level of truncation is the same for all basis sets. It is important to note also that for larger systems (of size greater than about $N=7$ or 8), it is generally only possible to perform truncated CI calculations and the truncation error is then central to the overall accuracy of the method.

B. Open-shell systems

Full CI calculations for the ground state of the $N=4$ electron dot are given in Table II. These results have been calculated with two basis-set potentials: a "configuration-averaged" HF potential[41] and the analytical potential $U(w,r)$

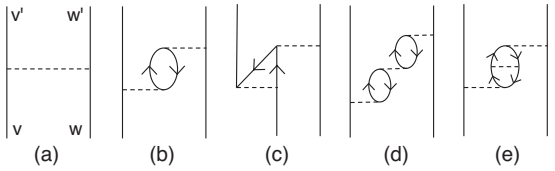

FIG. 2. Sample goldstone diagrams through third order for the interaction of two valence electrons, corresponding approximately to the CI-singles approximation with a valence model space. The external legs v, w, v', and w' indicate valence electrons. Diagram (a) is the lowest-order interaction with the bare Coulomb interaction; (c) and (e) are sample exchange variants of (b) and (d), respectively.

of Eq. (13). The configuration average for the HF potential is over all combinations of ℓ_z and spin of the outer incomplete valence shell, which ensures a circularly symmetric and spin-independent potential and thus yields good quantum numbers at each level of CI truncation. The model space is here constructed as described in Sec. II B, by choosing a $1s^2$ core and distributing the $(N-2)$ valence electrons in all possible ways among the $1p^4$ valence shell (subject to conservation laws for the z component of total spin S_z and orbital angular momentum L_z).

Table II illustrates a general feature of open-shell systems with a mean-field potential: while singles are small for the ground state of closed-shell systems (and zero for a HF potential), as we have noted above, they are enhanced for open-shell systems. Doubles are important, as for closed-shell systems, because they contribute the leading correlation effects for potentials of HF type. The relative enhancement of singles for open-shell systems is due in part to our choice of a spin-independent mean-field potential U, which has the consequence that the important physical effect of spin polarization enters in leading order in the singles contribution.

To see this in more detail, we show in Fig. 2 the approximate equivalent within many-body perturbation theory (MBPT) of the present open-shell CI-singles approximation.[43,44] The singles approximation includes an infinite subset of diagrams with loops to all orders, together with their exchange variants such diagrams contain only single excitations in the intermediate states. At least two basic physical effects are thus accounted for within our model space treatment of singles. First, the screening of the Coulomb interaction between those valence electrons included in the definition of the model space due to polarization of the core (here, particle-hole excitations from the $1s^2$ core). Second, because of the spin dependence of the exchange diagrams, we incorporate the leading spin-polarization effects.[41]

Note that we could have included spin polarization in lowest order by using a spin-polarized mean-field basis such as SDFT or unrestricted Hartree-Fock,[36] in which the mean field U is spin dependent and the single-particle states of spin-up and spin-down electrons can differ. However, this would have the consequence that in general, for an arbitrary truncation of CI, the states will not be eigenstates of total spin $\mathbf{S}^2$, and nor will the $(2S+1)$ substates be degenerate to machine precision; these symmetries would be recovered only in the limit of full CI and basis-set completeness. This may lead to ambiguities if it is desired to determine the spin of the states. In the present approach, we include the leading effect of spin polarization at the level of single excitations, which is still a computationally very cheap calculation, but within a framework in which the total spin quantum number S remains exact at each level of truncation.

C. Excitation energies

A full CI calculation of the ground-state energy and first excitation energy of the $N=7$ electron dot is shown in Table III, for two different basis-set potentials. Here, we first calculate the excitation energy for several shell-index cutoffs n_{sh} (see Sec. III A), and only then extrapolate to the basis-set limit $n_{\mathrm{sh}} \to \infty$. Extrapolating in this order results in errors in the excitation energy that are typically an order of magnitude less than the errors in individual total energies. In general, the relative contributions to excitation energies can be quite

TABLE III. Contributions to the ground-state energy and first excitation energy of the $N=7$ electron circular parabolic dot with density parameter $\lambda=1.89$ ($r_s \approx 1.7 a_0^*$). HF-av denotes a configuration-averaged Hartree-Fock basis set, $w=0.75$ a basis-set in the potential of Eq. (13) with that value of w.

	Ground state (^2D) [Ha*]		Excitation energy ($^2S-^2D$) [mHa*]	
Excitation	HF-av	$w=0.75$	HF-av	$w=0.75$
LO-CI	10.526	10.770	50.4	78.8
Singles	−0.089	−0.333	−17.2	−26.2
Doubles	−0.320(2)	−0.273(2)	0.0(4)	−12.8(2)
Triples	−0.044	−0.091	−4.7(2)	−10.6
Quadruples	−0.038(2)	−0.038(4)	−4.6(1)	−4.6(2)
Pentuples	−0.004(1)	−0.008(1)	−0.3(1)	−1.2(4)
Hextuples	−0.001	−0.001	−0.4(1)	−0.1
Septuples	0.000	0.000	0.0	0.0
TOTAL	10.029(3)	10.027(5)	23.1(5)	23.3(5)
Ref. 20 (QMC)	10.0342(1)		27.5(1)	

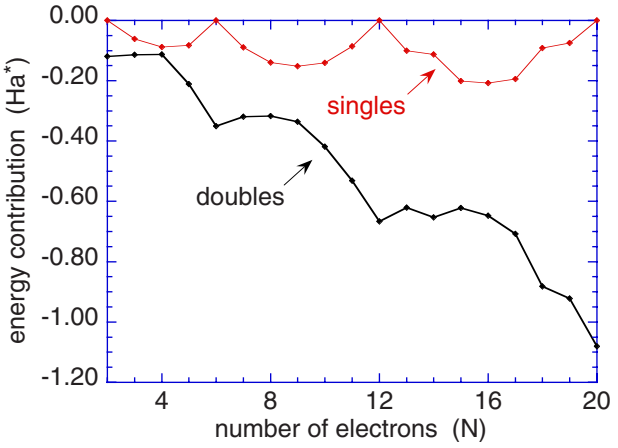

FIG. 3. (Color online) Singles and doubles contributions to the ground-state energy of parabolic dots for density parameter $\lambda = 1.89$ and a configuration-averaged HF basis (see text).

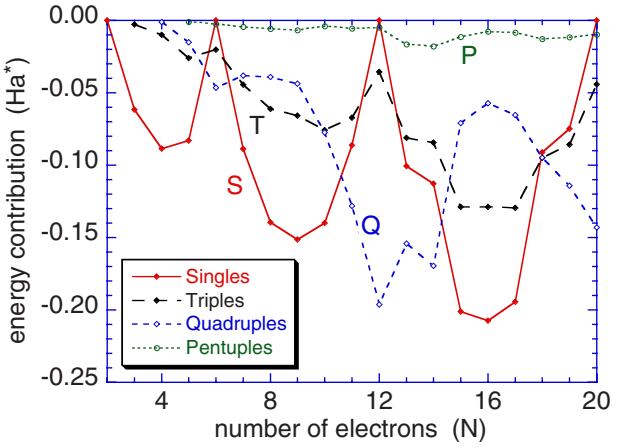

FIG. 4. (Color online) Singles, triples, quadruples, and pentuples contributions to the ground-state energy of parabolic dots for density parameter $\lambda = 1.89$ and a configuration-averaged HF basis (see text).

important for all excitations up to quadruples, but tend to show convergence for higher degrees of excitation (at least, for $2 \leq N \leq 20$).

IV. CORRELATION ENERGY $2 \leq N \leq 20$

In this section, we apply our CI method systematically to dots containing $2 \leq N \leq 20$ electrons at densities around $r_s \approx 1.7 a_0^*$, which occur in many experiments. In order to have a point of comparison, we choose the same electron densities as have been used in a complete and precise QMC study of small quantum dots by Pederiva *et al.*,[20] who report statistical errors of order 0.1 mHa* in ground-state energies using a variational-diffusion quantum Monte Carlo (VMC/DMC) approach. The first phase of their method is a variational Monte Carlo (VMC) calculation, after which the energies and wave functions are refined by a second phase of diffusion Monte Carlo (DMC). During the DMC phase, the nodes of the many-body wave function are held fixed (at the positions given by the final VMC wave function), in order to improve the convergence of the Monte Carlo process for fermionic systems. The final DMC phase may be regarded as giving a variational upper bound to the energy, containing a systematic error if there is some inaccuracy in the assumed positions of the nodes. While the statistical error in the Monte Carlo process is relatively easy to compute, the systematic fixed-node error is harder to estimate, but is expected to be small.[20]

We include in our CI calculation all the states considered in Ref. 20 along with several others, for a density parameter $\lambda = 1.89$. Here $\lambda = l_0/a_0^*$ is the ratio of the confinement length scale $l_0 = \sqrt{\hbar/m^*\omega}$ to the effective Bohr radius; it is related to the Wigner-Seitz radius r_s defined in Eq. (11) by $r_s^3 = \lambda^4/\sqrt{N}$ (in effective atomic units), so that for this range of N we have $r_s \approx 1.4-2.1 a_0^*$. The calculation for $2 \leq N \leq 7$ can proceed by full CI, but for higher N it is necessary to limit the number of Slater determinants included by using truncated CI. We include up to hextuple excitations for $N = 8, 9$ and up to pentuple excitations for $10 \leq N \leq 20$.

The model space is generated as described in Sec. II B by taking the core as the largest contained closed-shell system ($N_c = 2$, 6, or 12) and distributing the valence electrons over the whole of the outer harmonic oscillator shell. (For example, for $N = 16$ we take $N_c = 12$ and distribute the four valence electrons over the $1f^4$ and $2p^4$ states, subject to symmetry constraints.) The results are checked by performing all calculations with at least two different basis-set potentials: the HF potential and the analytical potential $U(w,r)$ of Eq. (13) with $w = 0.75$ or 1. For open-shell systems, the HF potential is here configuration-averaged (as in Sec. III B) over all l_z and spins of the final open valence shell or shells. (For example, for $N = 14$ with valence configuration $1f^2$, we configuration-average the two valence electrons over the $1f^4$ states. For $N = 16$ with a nominal valence configuration $1f^2 2p^2$ from Hund's rule,[7] we configuration average all four valence electrons over the $1f^4 2p^4$ states.) In all cases, the final results with different potentials agree to within the estimated error from the extrapolation to the basis-set limit, which provides a useful check on the calculation.

The maximum upper shell-index cutoff n_{sh} (see Sec. III A) considered in the single-particle basis sets, before extrapolation to the basis-set limit $(1/n_{\mathrm{sh}}) \to 0$, are as follows. We define the shell index of the lowest $1s$ (harmonic oscillator) shell to be $n_{\mathrm{sh}} = 1$, that of the $1p$ shell to be $n_{\mathrm{sh}} = 2$, etc. For the singles and doubles contributions, we calculate up to $n_{\mathrm{sh}} = 18$. For triples, we consider up to $n_{\mathrm{sh}} = 14$ for $3 \leq N \leq 7$, up to $n_{\mathrm{sh}} = 12$ for $8 \leq N \leq 12$, and up to $n_{\mathrm{sh}} = 10$ for $13 \leq N \leq 20$. For quadruples, we consider up to $n_{\mathrm{sh}} = 10$ for $4 \leq N \leq 6$, and up to $n_{\mathrm{sh}} = 8$ for $7 \leq N \leq 20$. For pentuples, we consider up to $n_{\mathrm{sh}} = 8$ for $5 \leq N \leq 12$ and up to $n_{\mathrm{sh}} = 6$ for $13 \leq N \leq 20$. For hextuples, we consider up to $n_{\mathrm{sh}} = 8$ for $6 \leq N \leq 8$ and up to $n_{\mathrm{sh}} = 7$ for $N = 9$.

We consider first the relative contribution of all excitations up to pentuples to the ground-state energy for the HF-type potentials. Figure 3 shows singles and doubles. As mentioned in Sec. III B, singles are zero for closed-shell systems but rise to a largest (most negative) value in the midshell

region, since in the present formalism singles account for the leading order of spin polarization. The doubles have a strong linear trend in this size range, with superposed shell structure.

Figure 4 shows triples, quadruples, and pentuples. As mentioned in Sec. III A, triples and quadruples tend to be comparable for a mean-field basis (and they are also comparable to singles). However, we see that pentuples are somewhat smaller. We have also calculated hextuples for $N=6-9$, finding them to be of order 8%–15% of pentuples for $N=8,9$. This suggests that there may be a significant drop between pentuples and hextuples at larger N also, where we truncate at pentuples.

The final ground-state and excitation energies are given in Table IV. As an informal estimate of the CI truncation error (for $N \geq 8$), we give in this table the size of the contribution of the highest-degree excitation included in the calculation. This contribution is in all cases somewhat smaller than the estimated error due to the extrapolation to the basis-set limit. In this sense, our level of CI truncation and our treatment of basis-set completeness are roughly consistent. A further confirmation of this is provided by the observation that calculations with different basis-set potentials give results agreeing to within the estimated error for extrapolation to the basis-set limit. Of the extrapolation errors, the quadruples extrapolation tends to be the most difficult, and thus contributes the dominant error to the whole calculation for most of the results presented. Overall, the CI calculation becomes less accurate as N increases, both because the number of Slater determinants increases rapidly with N for a given shell-index cutoff n_{sh} (see Sec. III A), and because the basis-set truncation error associated with a given value of n_{sh} also increases with N. (See Ref. 45 for a discussion of convergence issues in analogous CI calculations of three-dimensional jellium clusters.)

In comparing our CI results with the VMC/DMC results of Pederiva *et al.*,[20] we note first that the error we have achieved in the CI calculation is up to 1–2 orders of magnitude greater (worse) than the statistical error in the VMC/DMC calculation. However, there are discrepancies in the ground-state energies for some of the small systems with $N \leq 7$ of order a few mHa* ($N=2$ and 4 are exceptions). The differences of ground-state energies given by the two calculations are plotted in Fig. 5. The discrepancy is clearest for $N=3$ (which has been verified by use of several different basis-set potentials). There are further discrepancies of order a few mHa* in a substantial number of the excitation energies, where our errors are up to an order of magnitude better than for the ground-state energies. We show in Table III an example of such a case, for the first excitation energy of the $N=7$ dot, together with the convergence pattern for two different basis-set potentials.

The cause for these discrepancies needs to be investigated more fully, but we note that since our discrepant ground-state energies are lower (more negative) than those of the VMC/DMC method, it is possible that we have revealed the systematic error in the VMC/DMC calculation due to the fixed-node approximation. This may also be the explanation for the discrepancies in the excitation energies, which are also of order a few mHa*. If this is true, it may be possible to improve the fixed-node error in the VMC/DMC approach of Ref. 20 by using an improved trial function in the VMC phase.

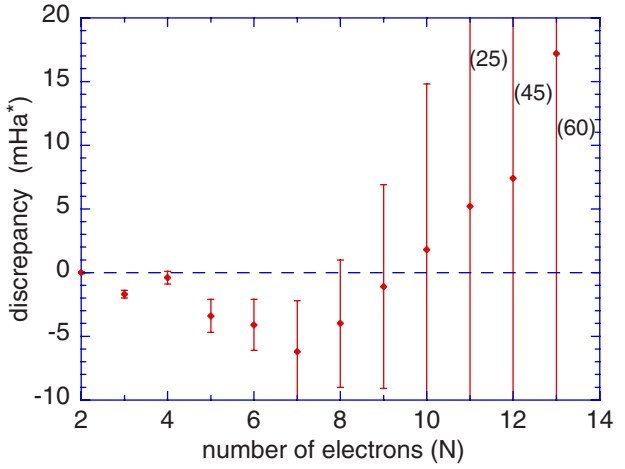

FIG. 5. (Color online) Discrepancy in ground-state energies between the present CI calculation and the VMC/DMC approach of Pederiva *et al.* (Ref. 20). Plotted are present results minus those of Ref. 20. Error bars indicate the error in the CI results arising from the extrapolation to the basis-set limit. The size of the error for $N=11$, 12, and 13 is 25, 45, and 60 mHa*, respectively.

Turning to the larger systems with $N>8$, we see from Table IV that the error in our CI calculation varies from about 8 mHa* ($N=9$) to about 110 mHa* ($N=20$). In this size range, the VMC/DMC approach may be more accurate, if one assumes that any fixed-node error that may be present is no greater than a few mHa*.

However, we note that the VMC/DMC method can only be used for the ground state or, more generally, for the lowest-energy state of a given symmetry (L_z,S), while CI is in principle capable of treating all excited states. For instance, for $N=9$ (Table IV, there are two states with $(L_z,S)=(0,1/2)$, and two with $(L_z,S)=(2,1/2)$, that may be formed within the valence model space; the VMC/DMC method is only capable of treating the lower-energy state of each pair. Thus, a CI approach can have important uses on these larger systems as well.

V. CONCLUSIONS

We have described a CI approach using a numerical mean-field basis set, which is generated and stored on a 2D Cartesian grid prior to the CI calculation. The CI calculations were organized hierarchically with respect to degree of excitation and extrapolated to the basis-set limit. For high electronic densities ($r_s \approx 1.7a_0^*$), the method gave errors ranging from 0.3 mHa* for $N=3$, to a few mHa* for $N=5-9$, and rising to about 100 mHa* for $N=20$. It should be noted, however, that convergence becomes more difficult in the low density, strongly interacting regime; we are currently extending the method for use in this regime.

Several improvements are possible to the present CI approach. One can gain in memory requirements by reevaluating the matrix elements of H_{CI} on the fly as they are required,

TABLE IV. Ground-state energies (E) and excitation energies (ΔE) given by the present CI approach for circular parabolic dots with density parameter $\lambda=1.89$, using full CI for $2\leq N\leq 7$, up to hextuple excitations for $N=8,9$, and up to pentuple excitations for $10\leq N\leq 20$. The error in parentheses on E or ΔE is the estimate of error in the extrapolation to the basis-set limit; the error $\delta\epsilon_{\mathrm{CI}}$ in brackets indicates the size of the highest-degree excitation included (for truncated CI). Both errors apply to the last tabulated digit of E or ΔE; thus, 25.6(19) indicates an absolute error of 1.9. Ref. 20 is a VMC/DMC approach, and the error given in parentheses is the statistical error. Units: E in Ha* and ΔE in mHa*.

N	L_z	S	E or ΔE	$\delta\epsilon_{\mathrm{CI}}$	Ref. 20
2	0	0	1.02168(8)		1.02162(7)
3	1	1/2	2.2322(3)		2.2339(1)
	0	3/2	51.3(3)		
4	0	1	3.7141(5)		3.7145(1)
	2	0	39.3(2)		41.1(1)
	0	0	64.0(2)		66.3(1)
5	1	1/2	5.5304(13)		5.5338(1)
	0	1/2	75.4(7)		
6	0	0	7.596(2)		7.6001(1)
	1	1	97(2)		
7	2	1/2	10.028(4)		10.0342(1)
	0	1/2	23.2(5)		27.5(1)
8	0	1	12.686(5)	[1]	12.6900(1)
	2	1	19.7(10)	[1]	21.9(1)
	4	0	25.6(19)	[2]	27.5(1)
	0	0	28.7(23)	[1]	36.0(1)
	2	0	47.1(9)	[1]	56.1(1)
	1	2	72(2)	[1]	
	1	1	82(4)	[1]	
	0	0	89(4)	[2]	
	3	1	97(2)	[1]	
9	0	3/2	15.579(8)	[1]	15.5801(1)
	2	1/2	19(3)	[0]	28.5(1)
	4	1/2	37(5)	[1]	42.6(1)
	0	1/2	43(5)	[1]	55.1(1)
	0	1/2	52(9)	[1]	
	2	1/2	69(6)	[0]	
10	2	1	18.725(13)	[4]	18.7232(1)
	0	0	0(3)	[1]	2.9(1)
	0	1	20.5(30)	[6]	23.3(1)
	2	0	37(3)	[1]	40.0(1)
	4	0	44(3)	[0]	46.7(1)
	0	0	66(9)	[2]	
11	0	1/2	22.079(25)	[6]	22.0738(1)
	2	1/2	16(4)	[1]	15.3(1)
	1	1/2	96(11)	[10]	
12	0	0	25.643(45)	[5]	25.6356(1)
	1	1	143(34)	[22]	
13	3	1/2	29.511(60)	[16]	29.4938(1)
	1	1/2	39(4)	[2]	39.2(1)
14	0	1	33.57(6)	[2]	
15	1	3/2	37.91(4)	[1]	
16	0	2	42.39(6)	[1]	

TABLE IV. (*Continued.*)

N	L_z	S	E or ΔE	$\delta\epsilon_{\mathrm{CI}}$	Ref. 20
17	3	3/2	47.09(6)	[1]	
18	0	1	51.95(8)	[1]	
19	1	1/2	57.05(9)	[1]	
20	0	0	62.25(11)	[1]	

rather than storing them in run-time memory. Also, our approach to truncating the number of Slater determinants included has been based on the degree of excitation from a lowest-order model space. It is likely that one may make further progress by employing a more intelligent selection of configurations. One such example is the use of "importance truncations" methods.[45]

ACKNOWLEDGMENTS

We gratefully acknowledge support from the Indo-French Center for the Promotion of Advanced Research (IFCPAR)/ Centre Franco-Indien pour la Promotion de la Recherche Avancée (CEFIPRA) under contract No. 3104-2.

*steven.blundell@cea.fr
†kavitaj@unipune.ernet.in

[1] L. Jacak, P. Hawrylak, and A. Wójs, *Quantum Dots* (Springer, Berlin, 1998).
[2] T. Chakraborty, *Quantum Dots—A Survey of the Properties of Artificial Atoms* (North Holland, Amsterdam, 1999).
[3] H. Grabert and M. H. Devoret, *Single Charge Tunneling: Coulomb Blockade Phenomena in Nanostructures, NATO Advanced Studies Institute, Series B: Physics* (Plenum, New York, 1992), Vol. 294.
[4] U. Meirav, M. A. Kastner, and S. J. Wind, Phys. Rev. Lett. **65**, 771 (1990).
[5] M. A. Reed, J. N. Randall, R. J. Aggarwal, R. J. Matyi, T. M. Moore, and A. E. Wetsel, Phys. Rev. Lett. **60**, 535 (1988).
[6] B. Su, V. I. Goldman, and J. E. Cunningham, Science **255**, 313 (1992).
[7] S. M. Reimann and M. Manninen, Rev. Mod. Phys. **74**, 1283 (2002).
[8] G. Bastard, *Wave Mechanics Applied to Semiconductor Heterostructures* (Les Editions de Physique, Les Ulis, France, 1998).
[9] C. Yannouleas and U. Landman, Phys. Rev. Lett. **82**, 5325 (1999).
[10] A. Emperador, E. Lipparini, and L. Serra, Phys. Rev. B **73**, 235341 (2006).
[11] M. Koskinen, M. Manninen, and S. M. Reimann, Phys. Rev. Lett. **79**, 1389 (1997).
[12] D. G. Austing, S. Sasaki, S. Tarucha, S. M. Reimann, M. Koskinen, and M. Manninen, Phys. Rev. B **60**, 11514 (1999).
[13] S. A. Akbar and I. H. Lee, Phys. Rev. B **63**, 165301 (2001).
[14] E. Räsänen, H. Saarikoski, M. J. Puska, and R. M. Nieminen, Phys. Rev. B **67**, 035326 (2003).
[15] B. Pujari, K. Joshi, D. G. Kanhere, and S. A. Blundell, Phys. Rev. B **76**, 085340 (2007).
[16] W. M. C. Foulkes, L. Mitas, R. J. Needs, and G. Rajagopal, Rev. Mod. Phys. **73**, 33 (2001).
[17] F. Bolton, Phys. Rev. Lett. **73**, 158 (1994).
[18] A. Harju, V. A. Sverdlov, R. M. Nieminen, and V. Halonen, Phys. Rev. B **59**, 5622 (1999).
[19] R. Egger, W. Häusler, C. H. Mak, and H. Grabert, Phys. Rev. Lett. **83**, 462 (1999).
[20] F. Pederiva, C. J. Umrigar, and E. Lipparini, Phys. Rev. B **62**, 8120 (2000); **68**, 089901(E) (2003).
[21] A. Ghosal, A. D. Güçlü, C. J. Umrigar, D. Ullmo, and H. U. Baranger, Nat. Phys. **2**, 336 (2006).
[22] G. W. Bryant, Phys. Rev. Lett. **59**, 1140 (1987).
[23] P. A. Maksym and T. Chakraborty, Phys. Rev. Lett. **65**, 108 (1990).
[24] D. Pfannkuche, R. R. Gerhardts, P. A. Maksym, and V. Gudmundsson, Physica B **189**, 6 (1993).
[25] T. Ezaki, N. Mori, and C. Hamaguchi, Phys. Rev. B **56**, 6428 (1997).
[26] S. M. Reimann, M. Koskinen, and M. Manninen, Phys. Rev. B **62**, 8108 (2000).
[27] S. A. Mikhailov, Phys. Rev. B **66**, 153313 (2002).
[28] R. M. Abolfath and P. Hawrylak, J. Chem. Phys. **125**, 034707 (2006).
[29] M. Rontani, C. Cavazzoni, D. Bellucci, and G. Goldoni, J. Chem. Phys. **124**, 124102 (2006).
[30] B. S. Pujari, K. Joshi, D. G. Kanhere, and S. A. Blundell, Phys. Rev. B **78**, 125414 (2008).
[31] T. M. Henderson, K. Runge, and R. J. Bartlett, Chem. Phys. Lett. **337**, 138 (2001).
[32] T. M. Henderson, K. Runge, and R. J. Bartlett, Phys. Rev. B **67**, 045320 (2003).
[33] I. Heidari, S. Pal, B. S. Pujari, and D. G. Kanhere, J. Chem. Phys. **127**, 114708 (2007).
[34] A. Emperador, E. Lipparini, and F. Pederiva, Phys. Rev. B **72**, 033306 (2005).
[35] A. Szabo and N. Ostlund, *Modern Quantum Chemistry* (Dover, New York, 1996).
[36] R. G. Parr and W. Yang, *Density-Functional Theory of Atoms and Molecules* (Oxford University Press, New York, 1989).
[37] W. H. Press, S. A. Teukolsky, W. T. Vetterling, and B. P. Flannery, *Numerical Recipes*, 2nd ed. (Cambridge University Press, Cambridge, 1992).
[38] G. H. Golub and C. F. Van Loan, *Matrix Computations*, 3rd ed.

(Johns Hopkins University Press, Baltimore, 1996).
[39] E. R. Davidson, J. Comput. Phys. **17**, 87 (1975).
[40] R. N. Barnett and U. Landman, Phys. Rev. B **48**, 2081 (1993).
[41] I. Lindgren and J. Morrison, *Atomic Many-Body Theory* (Springer, Berlin, 1986).
[42] R. J. Bartlett and M. Musiał, Rev. Mod. Phys. **79**, 291 (2007).
[43] Such Goldstone diagrams would occur as "two-body" terms in the open-shell Fock-Space version of MBPT described in Ref. 41. There are also diagrams corresponding to modifications of the core energy and the "one-body" valence energies, which we have not shown. The correspondence of this MBPT formalism with our open-shell CI singles is not a formally exact one, but it is close.
[44] M. Koskinen, M. Manninen, and P. O. Lipas, Phys. Rev. B **49**, 8418 (1994).
[45] R. Roth, Phys. Rev. C **79**, 064324 (2009).